Journal of Organometallic Chemistry 927 (2020) 121514

Contents lists available at ScienceDirect

Journal of Organometallic Chemistry

journal homepage: www.elsevier.com/locate/jorganchem

Synthesis of Luminescent 2-7 Disubstituted Silafluorenes with alkynyl-carbazole, -phenanthrene, and -benzaldehyde substituents

Stephan Germann, Shelby J. Jarrett, Cynthia M. Dupureur, Nigam P. Rath, Ethan Gallaher, Janet Braddock-Wilking*

Department of Chemistry and Biochemistry and Center for Nanoscience, University of Missouri St Louis, St. Louis, Missouri 63121, United States

ARTICLE INFO

Article history:
Received 15 June 2020
Revised 5 September 2020
Accepted 7 September 2020
Available online 20 September 2020

ABSTRACT

Three new fluorescent 2,7-alkynyl(aryl)-3,6-dimethoxy-9,9-diphenylsilafluorenes have been synthesized using a Pd-catalyzed Sonogashira coupling reaction to incorporate alkynyl(aryl) groups at the 2,7-positions of the ring. The substituents include 9-ethynylcarbazole, 4-ethynylbenzaldehyde, and 3-ethynylphenanthrene. These new compounds were characterized utilizing X-ray crystallography as well as multinuclear NMR, mass spectrometry, UV-Vis, and fluorescence spectroscopic techniques. These silafluorenes, which are yellow crystals in the solid state, showed high quantum yields with moderate molar extinction coefficients in dichloromethane and strong blue emission. Key words: silafluorene, luminescence.

1. Introduction

Silafluorene ring systems, also known as dibenzosiloles and the related silacyclopentadienes (silole), are a class of molecules that demonstrate intense fluorescent emission that arises from the σ^*-π^* conjugation between the exocyclic groups at the silicon center and the butadiene unit of the ring resulting in a low-lying LUMO energy level [1,2]. Theoretical studies on 9-heterofluorenes with Si, Ge, N, P, O, S or B in the 9-position of the ring showed that these molecules are highly aromatic and electrooptically active [3]. Silafluorenes have been shown to exhibit fluorescence both in solution and in the solid state making them useful molecules for a number of applications. For example, silafluorenes have been reported as host materials for a blue phosphorescent OLED, a red phosphorescent OLED, and a blue to deep-blue OLED, respectively [4–6]. Silafluorene based compounds have also been used as chemical sensors, such as in the detection of explosive materials such as TNT [7].

Silafluorenes have also been studied extensively in applications for photovoltaic cells. A silafluorene and a related spirosilafluorene compound containing substituted triphenylamine groups at the 2,7-positions have been studied for photovoltaic applications as a hole transporting material in perovskite solar cells [8]. Three novel dibenzosilole D-π-A sensitizers were synthesized for components in dye-sensitized solar cells [9]. Also, a push-pull red-emitting 2-amino-7-acceptor-9-silafluorene fluorophore was synthesized and found to be highly efficient for solar concentrators [10]. A 2,7-bis-aryl(alkoxy)silafluorene and a related spiro-bridged silafluorene were reported and found to exhibit high thermal stability and liquid crystal behavior [11].

There have been a few reports of the involvement of silafluorenes in biochemical related applications. A silafluorene linked to a [FeFe]-hydrogenase was prepared for photolytic [FeFe]-H^2ase mimic where the silafluorene moiety serves as a photosensitizer [12]. A silafluorene molecule with a hexafluoro-2-hydroxypropyl group on the aromatic ring was synthesized and studied as a novel ROR inverse agonist [13]. Poly(2,7-dibenozosilole) was studied as a fluorescent label for biomolecules for antibody-based flow cytometry [14]. These examples demonstrate the broad applications of optically active silafluorenes and their tunability due to various substituted groups.

Related 2,7-dibromosilafluorene derivatives with different substituents at the silicon center have been synthesized [15]. A number of new synthetic routes have been reported for the synthesis of fluorescent silafluorene molecules. Yamanoi and Nishihara reported the cyclic double intramolecular arylation reaction of a 2,2'-diiodobiaryl with a secondary silane, an added base and a Pd catalyst to form a series of silafluorenes and germafluorenes in high yield [16]. Takai et al. reported a rhodium-catalyzed reaction of biphenylhydrosilanes to prepare a series of silafluorenes and related silicon ring systems [17]. Holthausen and Lerner et al. synthesized substituted silafluorenes using diethylsilane and

* Corresponding author.
E-mail address: wilkingj@umsl.edu (J. Braddock-Wilking).

https://doi.org/10.1016/j.jorganchem.2020.121514
0022-328X/

biphenylenes in the presence of a nickel catalyst [18]. Chen, Lei, Knochel, and coworkers carried out cyclolanthanation reactions to synthesize polyfunctionalized diiodobiaryl derivatives which were used to prepare new silafluorenes, fluoren-9-ones, phenanthrenes, and other related heterocyclic compounds [19]. Nozaki and Shintani et al. reported a Rh-catalyzed asymmetric synthetic route to dibenzosiloles via an enantioselective [2+2+2] cycloaddition reaction [20]. A series of 13 new 9-silafluorenes as well as several related ring systems were synthesized utilizing a base-promoted homolytic aromatic substitution [21]. Dibenzosiloles functionalized at one or both aromatic rings were prepared from ortho-silylated biphenyls via an intramolecular electrophilic aromatic substitution pathway [22]. A series of silafluorenes and silaindenes were prepared by an intramolecular homolytic aromatic silylation reaction involving biphenyl-2-hydrosilanes and silyl radicals [23]. Murata and co-workers carried out Pt-catalyzed intramolecular dehydrogenative cyclization reactions of 2-(dialkylsilyl)biaryls to produce a series of silafluorene derivatives [24]. He and coworkers investigated the preparation of several silafluorene derivatives and related ring systems by a rhodium-catalyzed route involving an intramolecular C-H silylation step with silacyclobutane [25]. A double sila-Friedel-Crafts reaction was utilized by Kuninobu and coworkers in the Lewis acid-catalyzed preparation of silafluorenes starting from biphenyl ring systems and dihydrosilanes [26]. A series of 9,9-dimethyl-9-silafluorenes silafluorenes were synthesized and functionalized through a sequence of reactions involving borylation, bromination and nitration [27]. A group of silafluorene derivatives were prepared by a Lewis-acid catalyzed reaction involving dihydrosilanes and aminobiphenyl derivatives in the presence of a borane catalyst [26].

Blue hyperfluorescent systems that exhibit thermally activated delayed fluorescence (TADF) are of interest as nondoped organic OLEDs. A similar framework to the compounds proposed here was investigated by Rao and coworkers that had a 9,9-dimethylacrinidine and fluorene-based donor-acceptor with a thioxanthene dioxide blocking unit [28]. Their compound showed moderate quantum efficiency and achieved solid state TADF due to the blocking unit. Two spiro-linked benzosilole moieties have been demonstrated in the literature by Xu and coworkers as a silicon containing PLED with a photoluminescence quantum yield of 0.84 [29]. Xu and coworkers also reported the synthesis of a deep-blue emitting polymer with a spiro-dibenzoazasiline system that was linked to a poly(dibenzosilole) moiety resulting in deep-blue emission for applications in power-efficient PLEDs [30].

2. Results and discussion

We previously reported the synthesis of a series of six 2,7-bis-alkynyl(aryl)-3,6-dimethoxy-9,9-diphenylsilafluorenes utilizing the precursor, 9,9-diphenyl-2,7-dibromo-3,6-dimethoxysilafluorene **1** [31]. Herein, we report the synthesis and characterization of three new silafluorene compounds containing alkynyl(aryl) substituents at the 2,7-positions of the silafluorene ring using a Sonogashira coupling reaction. The new aryl groups used in the current study are based on phenanthrene, benzaldehyde, and carbazole. All silafluorenes were observed to have strong blue emission in solution, with tunability conferred by the alkynyl(aryl) groups. These new compounds were characterized using X-ray crystallography, multinuclear NMR, mass spectrometry, UV-Vis, and fluorescence spectroscopic techniques and are discussed herein.

2.1. Synthesis and characterization

The precursor compound needed to make the required 2,7-dibromo-3,6-dimethoxysilafluorene described herein was

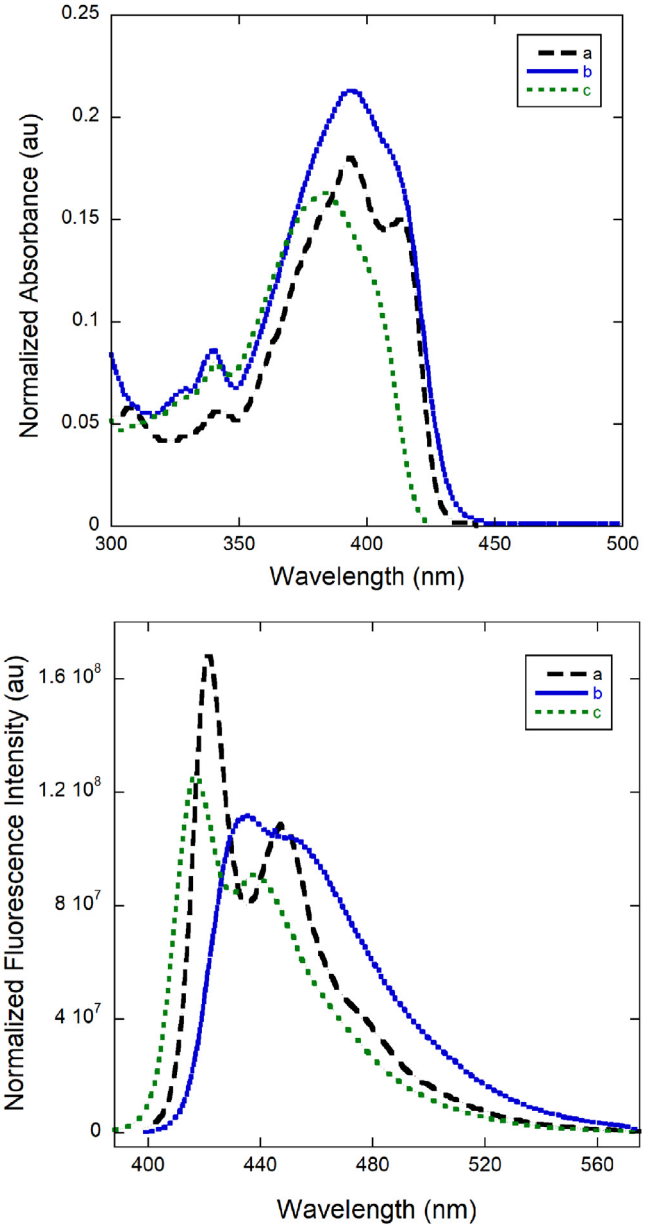

Fig. 1. Molecular structure of **2a**. Hydrogen atoms and solvent molecules have been removed for clarity. Thermal ellipsoids are drawn at the 50% probability level. Selected bond distances (Å), bond angles (deg), and angles between bonds (deg) for 2a: Si1-C1= 1.8600(19), Si1-C24 = 1.8630(18), Si1-C47 = 1.868(2), Si1-C53 = 1.870(2), C1-C2 = 1.415(2), C2-C3 = 1.392(3), C3-C4 = 1.392(3), C4-C5 = 1.418(3), C5-C6 = 1.397(3), C5-C7 = 1.439(3), C7-C8 = 1.172(3), C8-C9 = 1.439(3), C9-C10 = 1.451(3), C10-C11 = 1.409(3), C11-C12 = 1.360(3), C1-C6 = 1.388(2), C12-C13 = 1.404(3), O1-C4 = 1.355(2), O1-C23 = 1.435(2), O2-C27 = 1.363(2), O2-C46 = 1.426(2), C13-C14 = 1.370(3), C17-C18 = 1.380(3), C25-C26 = 1.398(2), C1-Si1-C47= 115.16(9), C24-Si1-C47= 114.98(9), C1-C2-C25= 114.38(16), C1-C6-C5= 121.61(17), C47-Si1-C53= 108.62(9), C1-Si1-C24= 91.52(8), C4-O1-C23= 117.48(15), C27-O2-C46= 116.74(15), C19-C10-C15-C14 =178.38(18), C15-C16-C21-C20= -177.30(18). Angles between bonds C29-C28 and C32-C45 = 119.3 deg; Angles between bonds C6-C5 and C9-C22 = 120.3 deg.

4,4'-dibromo-2,2'-diiodo-5,5'-dimethoxy-1,1'-biphenyl. The latter compound was prepared in two steps in high yield starting from commercially available *o*-dianisidine [32]. Reaction of 4,4'-dibromo-2,2'-diiodo-5,5'-dimethoxybiphenyl with *n*BuLi in THF followed by addition of diphenyldichlorosilane afforded the corresponding 2,7-dibromosilafluorene (**1**) in **76** % yield [15,31].

Moderate yields of **2a-c** were obtained using the procedure outlined by Hammerstroem et al. (2016) where silafluorenes **2a-c**

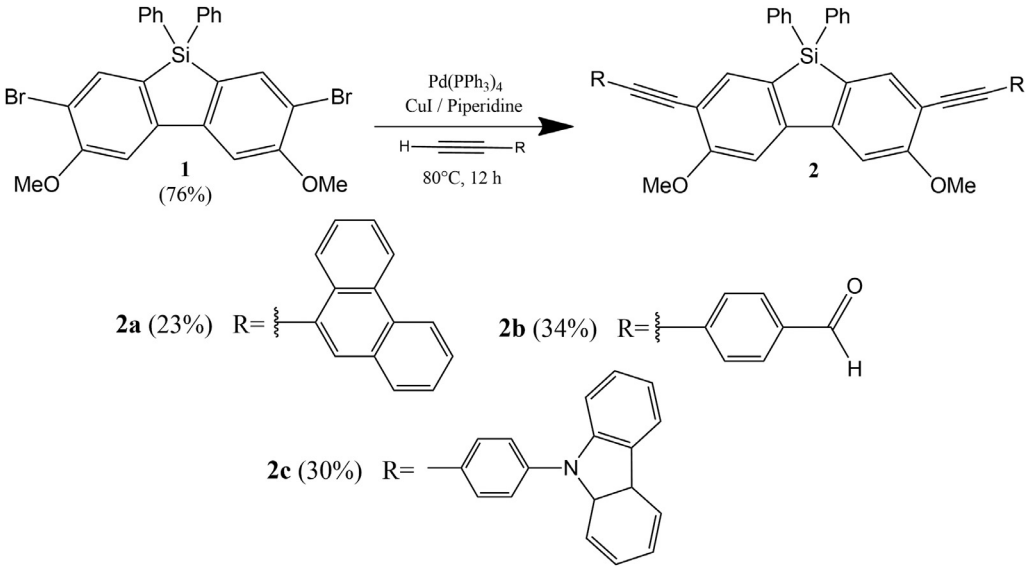

Scheme 1.

were prepared using Sonagashira cross-coupling conditions shown in Scheme 1 [31]. Compound **1** does not exhibit fluorescence in the solid state or in solution, however compounds **2a-c** exhibit fluorescence in the reaction mixture after stirring for 30 minutes at 80°C. Upon purification and recrystallization, the silafluorenes are yellow crystalline powders with moderate yields (23-34%, based on compound **1**). Compounds **2a-c** were characterized by ^{1}H NMR and ^{13}C{^{1}H} NMR where the spectra showed good agreement with related literature values for expected peaks. All three compounds **2a-c** were characterized by X-ray crystallography, multinuclear NMR spectroscopy, mass spectrometry, UV-Vis and fluorescence spectroscopy, quantum yield, and melting point.

2.2. X-ray Crystal Structures

X-ray quality crystals of silafluorenes **2a-c** were obtained as yellow needles. Several solvents were attempted for recrystallization of **2a** and small weakly diffracting crystals were obtained. X-ray data for **2a** were obtained from the Advanced Light Source (ALS) at the Lawrence Berkeley National Laboratory. Compound **2b** crystallized from slow evaporation from chloroform and some residual ethanol. Compound **2c** was crystallized from dichloromethane. The crystal structure contained a probable molecule of CH_2Cl_2 that could not be modeled well. Table 1 provides some crystallographic and data collection parameters for compounds **2a-c**.

Compounds **2a** and **2c** crystallized in the space group P1 whereas compound **2b** crystallized in the space group Pbca (Table 1). The molecular structures are shown in Figures 1, 2, and 3 for compounds **2a, 2b**, and **2c**, respectively along with selected bond distances and angles. The new compounds display similar X-ray structural data with respect to bond distances and angles to those previously reported [30,33]. The bond lengths for the Si-C bonds of the ring ranged from 1.855-1.871Å. The exocyclic silicon-carbon bond distances to the phenyl substituents were found to range from 1.862-1.871 Å. The carbon-carbon bond lengths in the five-membered silicon-containing ring ranged from 1.399-1.487 Å. The triple bond of the alkynyl unit for compounds **2a-c** were found to be in the range of 1.172-1.198 Å.

The X-ray crystal structures all exhibit a non-coplanar arrangement with respect to the central silicon-containing ring system and the aryl(alkynyl) substituents at the 2,7-positions (Figures 1-3). For compound **2a** the angles between bond sets C29-C28 and C32-C45 was found to be 119.3 degrees and angles between bonds sets C6-C5 and C9-C22 was similar at 120.3 degrees. For compound **2b** the angles between bonds C21-C20 and C29-C24 was 111.6 degrees and angles between bonds C6-C5 and C9-C14 was significantly larger at 135.4 degrees. Compound **2c** had angles between bonds C6-C5 and C9-C14 of 118.9 degrees and angles between bonds C31-C32 and C40-C35 of 110.1 degrees.

Table 1
Crystallographic and Data Collection Parameters for **2a-c**.

	2a[a]	2b	2c
Formula	$C_{58}H_{38}O_2Si$	$C_{44}H_{30}O_4Si$	$C_{66}H_{44}Cl_3N_2O_2Si$
fw	794.97	650.77	925.12
cryst syst	Triclinic	Orthorhombic	Triclinic
space group	P1	Pbca	P1
a, Å	12.0986(15)	21.582(3)	11.1852(5)
b, Å	12.5130(15)	8.3972(9)	12.9545(6)
c, Å	14.4986(18)	40.443(5)	19.5039(9)
α, deg	102.235(4)	90	109.285(3)
β, deg	101.989(4)	90	101.023(2)
γ, deg	98.442(4)	90	97.587(2)
V, Å^3	2056.1(4)	7329.6(15)	2559.5(2)
Z	2	8	2
d_{calc}, g/cm^3	1.284	1.179	1.200
μ, mm^{-1}	0.125	0.105	0.094
R1,[b] wR2[c]	0.0496, 0.1337	0.0608, 0.1668	0.0524, 0.1329
goodness-of-fit on F^2	1.007	1.295	1.022
CCDC Deposit #	2015348	2015350	2015349

[a] λ, = 0.71073 Å (Mo), T = -100(2) K.
[b] R1 = $(\Sigma||F_o| - |F_c||)/\Sigma|F_o|$. [c] wR2 = $[(\Sigma w(F_o^2 - F_c^2)^2)/\Sigma w(F_c^2)^2]^{1/2}$. All crystals were yellow needles.

2.3. Electronic Transitions

Absorbance spectra of compounds **2a-c** in dichloromethane appear in Figure 4 **(top panel)** and are plotted at the same concentration so differences in extinction coefficient are reflected. Compound **2b** absorbs most strongly, followed by **2a**. Compound **2a** exhibits sharper features than those exhibited by **2b** and **2c**. Compound **2b** exhibits the broadest spectra and could reflect solvent interactions between the polar benzaldehyde group and solvent. Finally, compound **2c** is the most blue-shifted. This could indicate that this compound self-associates in a way that protects the molecules from polar and/or solvent effects.

Fluorescence spectra in dichloromethane appear in Figure 4 **(bottom panel)** at identical concentrations. Trends

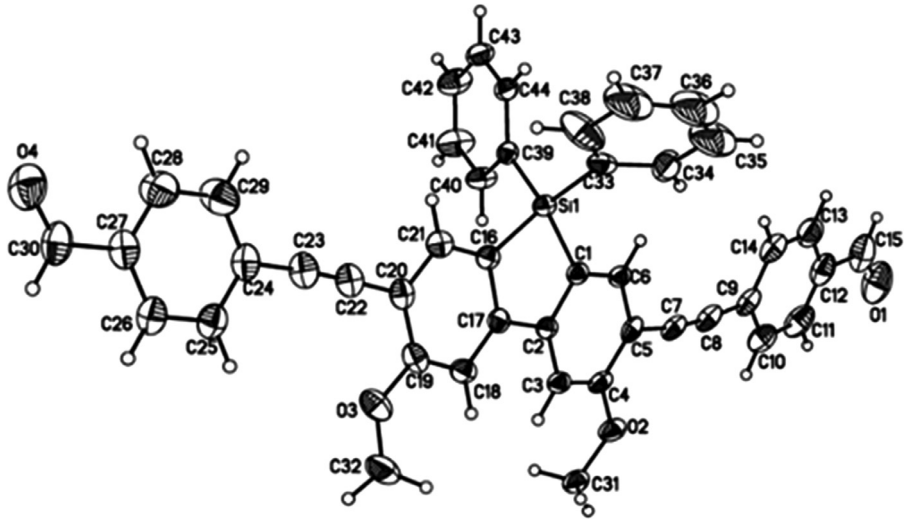

Fig. 2. Molecular structure of **2b**. Hydrogen atoms and solvent molecules have been removed for clarity. Thermal ellipsoids are drawn at the 50% probability level. Selected bond distances (Å), bond angles (deg), and torsion angles (deg) for 2b: Si1-C1 = 1.855(3), Si1-C16 = 1.858(3), Si1-C33 = 1.865(3), Si1-C39 = 1.865(2), C1-C2 = 1.407(3), C2-C3 = 1.393(3), C3-C4 = 1.383(4), C4-C5 = 1.410(4), C5-C6 = 1.393(4), C7-C8 = 1.198(4), C8-C9 = 1.424(4), C9-C10 = 1.388(4), C10-C11 = 1.389(4), C11-C12 = 1.383(5), C1-C6 = 1.381(3), C2-C17 = 1.482(3), O1-C15 = 1.216(5), O2-C4 = 1.355(3), O2-C31 = 1.426(3), C13-C14 = 1.379(4), C20-C22 = 1.427(4), C22-C23 = 1.195(4), C1-Si1-C16 = 91.47(11), C1-Si1-C33 = 114.07(11), C1-C2-C17 = 114.5(2), C12-C11-C10 = 120.6(3), C16-Si1-C33 = 112.50(12), C34-C33-Si1 = 121.5(2), O4-C30-C27 = 126.2(3), C4-O2-C31 = 117.1(2), C2-C17-C18-C19 = -177.8(2), C17-C2-C3-C4 = 177.1(2). Angles between bonds C21-C20 and C29-C24 = 111.6 deg; Angles between bonds C6-C5 and C9-C14 = 135.4 deg.

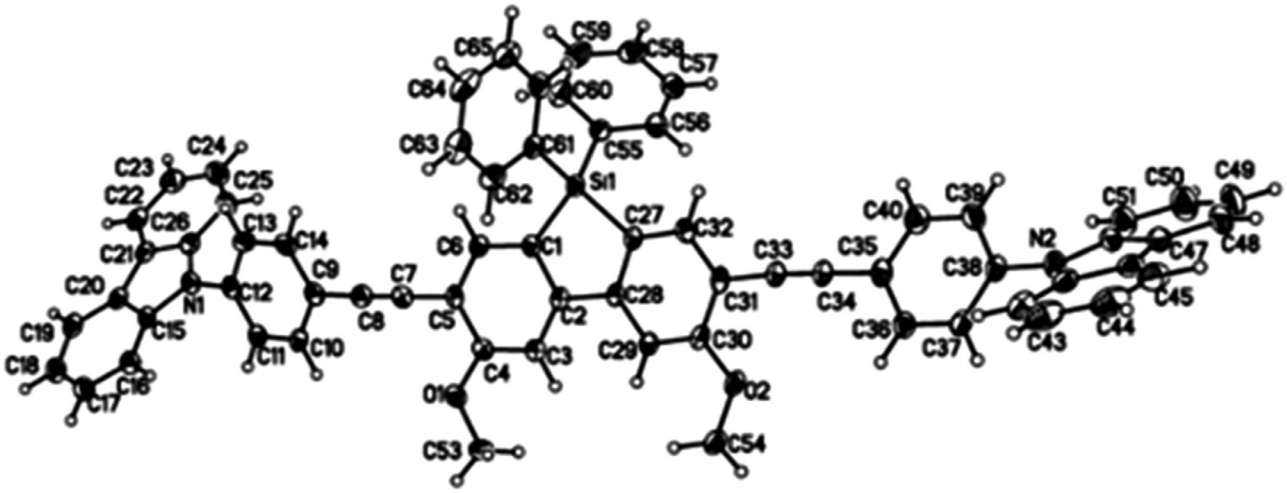

Fig. 3. Molecular structure of **2c**. Hydrogen atoms and solvent molecules have been removed for clarity. Thermal ellipsoids are drawn at the 50% probability level. Selected bond distances (Å), bond angles (deg), and torsion angles (deg) for 2c: Si1-C1 = 1.857(2), Si1-C55 = 1.862(2), Si1-C61 = 1.871(2), Si1-C27 = 1.871(2), C1-C2 = 1.404(3), C2-C3 = 1.394(3), C3-C4 = 1.389(3), C4-C5 = 1.407(3), C5-C6 = 1.396(3), C7-C8 = 1.175(3), C8-C9 = 1.441(3), C9-C10 = 1.392(3), C10-C11 = 1.383(3), C11-C12 = 1.377(3), C1-C6 = 1.390(3), N1-C15 = 1.396(3), O1-C4 = 1.354(3), O1-C53 = 1.432(3), O2-C30 = 1.360(3), O2-C54 = 1.424(3), N2-C52 = 1.388(3), C13-C14 = 1.383(3), N2-C38 = 1.422(3), C21-C22 = 1.399(3), C1-Si1-C55 = 115.73(10), C1-Si1-C27 = 91.83(10), C1-Si1-C61 = 110.65(10), C1-C2-C28 = 114.83(19), C10-C9-C8 = 121.5(2), C32-C27-Si1 = 132.68(18), C61-Si1-C27 = 115.19(10), C4-O1-C53 = 116.52(17), C30-O2-C54 = 117.51(18), C2-C3-C4-C5 = -0.2(3), C15-N1-C12-C13 = -130.2(2). Angles between bonds C6-C5 and C9-C14 = 118.9 deg; Angles between bonds C31-C32 and C40-C35 = 110.1 deg.

similar to the absorption spectra are observed. Compound **2b** has the broadest spectrum, and **2c** is the most blue-shifted. As summarized in **Table 2**, quantum yields in DCM are high but comparable to those published previously for other 2,7-disubstituted silafluorenes [31]. The quantum yields follow the trend **2a** > **2c** = **2b**, most likely due to the high amount of conjugation in **2a**. Concentration dependent fluorescence spectra for compounds **2a-c** are shown in **Figure S4-6** in Supplementary Materials.

In conclusion, three 2,7-disubstituted silafluorenes with alkynyl(aryl) substituents including phenanthrene (**2a**), benzaldehyde (**2b**), and carbazole (**2c**) were successfully synthesized starting from the 2,7-dibromosilafluorene precursor **1** followed by Pd-catalyzed Sonogashira coupling reactions to form products **2a-2c**. All three compounds were confirmed by X-ray crystallography and exhibit high quantum yields in organic solvent (above 85%) with blue emission maxima.

3. Experimental

3.1. General Procedures

Reactions were carried out under argon atmosphere using standard Schlenk techniques with solvents dried and purified by standard methods. Chloroform, dichloromethane, pentane, ethanol, and hexane were used as received. The compounds 3-ethynylphenanthrene, and 4-ethynylbenzaldehyde were purchased from Millipore Sigma and 9-(4-ethynylphenyl)-9H-carbazole was purchased from TCI America and used without further purifica-

Table 2
UV−Visible and Fluorescence Spectral Data for Silafluorenes 2a-c.

Compound	λ_{max} absorbance (nm)	ε (M^{-1} cm^{-1})	λ_{max} fluorescence (nm)	Φ_f [a]
2a	393	43,600	421	0.94 ± 0.018
2b	394	57,100	435	0.85 ± 0.003
2c	383	39,600	416	0.86 ± 0.019

[a] All measurements performed in CH_2Cl_2. Excitation at 350 nm with Coumarin 102 in ethanol as a standard. The Φ_F is the average value of repeated measurements with a 95% CI.

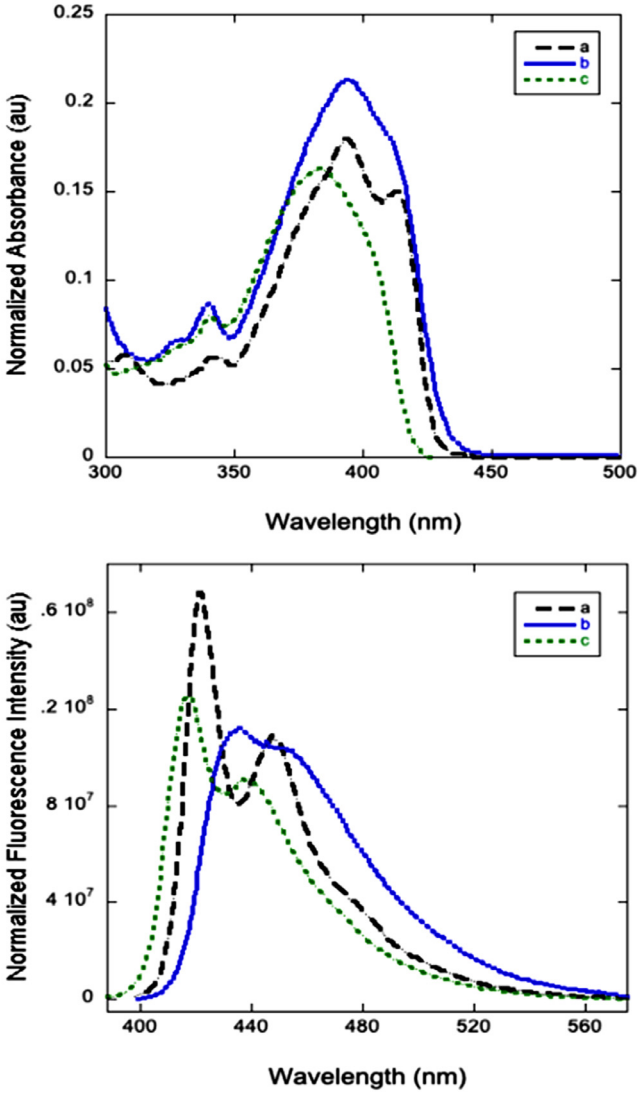

Fig. 4. top) Normalized UV/Vis and (bottom) fluorescence spectra of **2a-c** at 4 micromolar in CH_2Cl_2. Slits were 0.6 and excitation wavelength at lambda max as per Table 2.

tion. All NMR spectra were collected on an Agilent 600 MHz (^{1}H recorded at 600 MHz, ^{13}C at 151 MHz,) or on a Bruker Avance-300 MHz (^{1}H recorded at 300 MHz and ^{13}C at 75 MHz) at ambient temperature unless otherwise noted. Chloroform-d was purchased from Cambridge Isotopes, Inc. Mass spectral data (ESI) were collected on a Bruker Maxis Plus (maXis HD) quadrupole time-of-flight mass spectrometer.

Melting point determinations were obtained on a Mel-Temp melting point apparatus and are uncorrected. UV-vis and fluorescence spectra were measured on Shimadzu UV-1800 spectrometer and a Horiba Spectrofluorometer. Emission spectra were measured using the λ_{max} value for each compound as determined by the absorption spectra. A Bruker Maxis Plus Mass spectrometer was used for Electrospray MS measurements.

3.2. General procedure for preparation of 2,7-alkynyl(aryl)-3,6-dimethoxy-9,9-diphenylsilafluorenes

To a flame-dried 15 mL three-necked flask equipped with a reflux condenser and magnetic stirrer under argon, 2,7-dibromo-3,6-dimethoxy-9,9-diphenylsilafluorene, $Pd(PPh_3)_4$, and CuI were added, followed by piperidine and the arylalkyne. The reaction mixture was stirred at 80°C overnight, then concentrated and purified by silica gel chromatography using dichloromethane:hexane (1:1 ratio) as the eluent. The product was then recrystallized from dichloromethane/hexanes (1:1), then rinsed with hexanes, and dried by rotorary evaporation.

3.3. Preparation of 2,7-(3-ethynylphenanthrene)-3,6-dimethoxy-9,9-diphenylsilafluorene (2a)

The compound was prepared following the general procedure, using 0.2051 g (0.371 mmol) of 2,7-dibromo-3,6-dimethoxy-9,9-diphenylsilafluorene, 0.1871g (0.925 mmol) of 3-ethynylphenanthrene as the arylacetylene, 0.044 g (0.038 mmol) of $Pd(PPh_3)_4$, 0.0148 g (0.078 mmol) of CuI, and 4.2 mL of piperidine. The product was received as a bright yellow powder (0.0678 g, 23% yield). Mp: decomp. 355-357°C. ^{1}H NMR (600 MHz, $CDCl_3$) δ 8.76 – 8.63 (m, 6H), 8.10 (s, 2H), 8.03 (s, 2H), 7.88 (d, J = 7.8 Hz, 2H), 7.77 – 7.69 (m, 8H), 7.67 (t, J = 7.7 Hz, 2H), 7.60 (t, J = 7.5 Hz, 2H), 7.50 – 7.36 (m, 8H), 4.20 (s, 6H). ^{13}C{^{1}H} NMR (151 MHz, $CDCl_3$) δ 163.15, 150.36, 138.78, 138.68, 135.82, 135.69, 132.51, 131.74, 131.68, 131.55, 131.44, 130.49, 130.30, 128.82, 128.71, 128.50, 128.34, 127.56, 127.15, 122.84, 120.26, 113.32, 104.29, 104.14, 93.42, 91.15, 56.37. MS (ESI): Calcd. For $C_{58}H_{38}O_2Si$: 794.26, found 794.2595. **Figure S1** in Supplementary Materials shows the ^{1}H NMR spectra for **2a**.

3.4. Preparation of 2,7-(4-ethynylbenzaldehyde)-3,6-dimethoxy-9,9-diphenylsilafluorene (2b)

The compound was prepared following the general procedure, using 0.2559 g (0.463 mmol) of 2,7-dibromo-3,6-dimethoxy-9,9-diphenylsilafluorene, 0.1465 g (1.13 mmol) of 4-ethynylbenzaldehyde as the arylacetylene, 0.052 g (0.045 mmol of $Pd(PPh_3)_4$, 0.0184 g (0.097 mmol) of CuI, and 5.2 mL of piperidine. The product was received as a bright yellow powder (0.0903 g, 30% yield). Mp: decomp. 255°C. X-ray-quality crystals were obtained by slow evaporation of a dichloromethane solution of the product at room temperature. ^{1}H NMR (300 MHz, $CDCl_3$) δ 10.01 (s, 2H), 7.94 – 7.81 (m, 6H), 7.67 (dd, J = 11.8, 7.3 Hz, 8H), 7.54 – 7.30 (m, 8H), 4.10 (s, 6H). ^{13}C{^{1}H} NMR (75 MHz, $CDCl_3$) δ 191.56, 162.94, 150.67, 139.09, 135.58, 135.37, 132.16, 132.13, 130.52, 129.94, 129.65, 128.67, 128.38, 112.39, 104.20, 94.02, 90.62, 56.15. ^{29}Si NMR (119 MHz, $CDCl_3$) δ -12.320.

MS (ESI): Calcd. For $C_{44}H_{30}O_4Si$: 650.191, found 650.1908. **Figure S2** in Supplementary Materials shows the ^1H NMR spectra for **2b**.

3.5. Preparation of 2,7-(9-ethynylcarbazole)-3,6-dimethoxy-9,9-diphenylsilafluorene (2c)

The compound was prepared following the general procedure, using 0.2122 g (0.384 mmol) of 2,7-dibromo-3,6-dimethoxy-9,9-diphenylsilafluorene, 0.2524 g (0.944 mmol) of 9-ethynylcarbazole as the arylacetylene, 0.056 g (0.048 mmol) of $Pd(PPh_3)_4$, 0.0159 g (0.083 mmol) of CuI, and 4.1 mL of piperidine. The product was received as bright yellow needle-like crystals (0.1213 g, 34% yield). Mp: 295-300°C. X-ray-quality crystals were obtained by slow evaporation of a dichloromethane solution of the product at room temperature. ^1H NMR (300 MHz, $CDCl_3$) δ 8.15 (d, J = 7.7 Hz, 4H), 7.95 (s, 2H), 7.79 (d, J = 8.1 Hz, 4H), 7.70 (d, J = 7.0 Hz, 4H), 7.57 (d, J = 8.2 Hz, 4H), 7.43 (dd, J = 7.8, 4.5 Hz, 16H), 7.35 – 7.27 (m, 4H), 4.14 (s, 6H). $^{13}C\{^1H\}$ NMR (75 MHz, $CDCl_3$) δ 162.84, 150.35, 140.67, 139.01, 137.55, 135.66, 133.24, 132.37, 130.49, 128.56, 128.39, 126.90, 126.18, 123.65, 122.61, 120.49, 120.32, 112.80, 109.89, 104.14, 94.13, 87.34, 56.21. ^{29}Si NMR (119 MHz, $CDCl_3$) δ -11.141. MS (ESI): Calcd. For $C_{66}H_{44}Cl_3N_2O_2Si$: 924.32, found 924.3167. **Figure S3** in Supplementary Materials shows the ^1H NMR spectra for **2c**.

3.6. X-ray Structure Determination of (2a-c)

X-ray quality crystals of appropriate silafluorenes **2a-c** were obtained as yellow needles from slow evaporation from chloroform and ethanol (**2b**) or dichloromethane (**2c**). Several solvents were attempted for recrystallization of **2a**. resulting in small weakly diffracting crystals of **2a**.

Crystals were mounted on MiTeGen cryoloops in random orientations. Preliminary examination and data collection were performed using a Bruker X8 Kappa Apex-II system single crystal X-Ray diffractometer equipped with Oxford Cryostream LT devices for **2b** and **2c**. Data sets were collected using graphite monochromated Mo Kα radiation (λ= 0.71073 Å) from a fine focus sealed tube X-Ray source. Diffraction data for **2a** were collected at 150K on a D8 goniostat equipped with a Bruker PHOTON100 CMOS detector at Beamline 11.3.1 at the Advanced Light Source (Lawrence Berkeley National Laboratory) using synchrotron radiation tuned to λ=0.7749Å. Preliminary unit cell constants were determined with a set of 36 narrow frame scans. Typical data sets consist of combinations of ω and ϕ scan frames with typical scan width of 0.5° and counting time of 1 to 30 seconds/frame. The collected frames were integrated using an orientation matrix determined from the narrow frame scans. Apex II and SAINT software packages [34] were used for data collection and data integration. Analysis of the integrated data did not show any decay. Final cell constants were determined by global refinement of reflections harvested from the complete data set. Collected data were corrected for systematic errors using SADABS [34] based on the Laue symmetry using equivalent reflections.

Crystal data and intensity data collection parameters are listed in Table 1. Structure solution and refinement were carried out using the SHELXTL- PLUS software package [35]. The structures were solved and refined successfully in the space groups, Pbca for **2b** and P-1 for **2c** and **2a**. Full matrix least-squares refinements were carried out by minimizing $\Sigma w(F_o^2\text{-}F_c^2)^2$. The non-hydrogen atoms were refined anisotropically to convergence. All hydrogen atoms were treated using appropriate riding model (AFIX m3). The final residual values and structure refinement parameters are listed in Table 1. Platon-Squeeze [36] was used for removing solvent contributions which could not be modeled satisfactorily ($CHCl_3$ and EtOH in overlapping sites) in **2b** and CH_2Cl_2 in **2c**. Crystallization from various solvents and different conditions only resulted in small and weakly diffracting crystals for the compound **2a**. Therefore, diffraction data had to be collected using a synchrotron source.

Complete listings of positional and isotropic displacement coefficients for hydrogen atoms and anisotropic displacement coefficients for the non-hydrogen atoms, and bond lengths and angles and torsion angles are listed as supplementary material. Tables of calculated and observed structure factors are available in electronic format. These data can be obtained free of charge from The Cambridge Crystallographic data Center via the link hMp://www.ccdc.cam.ac.uk/data_request/cif using deposit numbers: 2015348, 2015350, and 2015349.

Acknowledgement: Funding from the National Science Foundation (CHE-1362431 to JBW) and (MRI, CHE-1827756 to NPR) for the purchase of the Venture-Duo diffractometer is acknowledged. Crystallographic data were collected for one of the structures through the SCrALS (Service Crystallography at Advanced Light Source) program at the Small-Crystal Crystallography Beamline 11.3.1 at the Advanced Light Source (ALS), Lawrence Berkeley National Laboratory. The ALS is supported by the U.S. Department of Energy, Office of Energy Sciences Materials Sciences Division, under contract DE-AC02-05CH11231.

ASSOCIATED CONTENT

Supporting Information. 1H NMR and concentration dependence of fluorescence spectra of 2a-c.

Declaration of Competing Interest

The authors declare that they have no competing financial interest or personal relationships that could have appeared to influence the results reported in this paper. Curators of the University of Missouri have been assigned all patent rights and have filed a patent application related to this technology.

Acknowledgment

We acknowledge funding from the National Science Foundation for support of this work (CHE-1362431). We also acknowledge funding from the National Science Foundation for the purchase of an Agilent DD2 600 MHz NMR spectrometer (MRI-0959360), for the purchase of an Apex-II diffractometer (MRI, CHE-0420497), and for funds to purchase a Venture-Duo diffractometer (MRI, CHE-1827756). Crystallographic data were collected for one of the structures through the SCrALS (Service Crystallography at Advanced Light Source) program at the Small-Crystal Crystallography Beamline 11.3.1 at the Advanced Light Source (ALS), Lawrence Berkeley National Laboratory. The ALS is supported by the U.S. Department of Energy, Office of Energy Sciences Materials Sciences Division, under contract DE-AC02-05CH11231.

Supplementary materials

Supplementary material associated with this article can be found, in the online version, at doi:10.1016/j.jorganchem.2020.121514.

References

[1] S. Yamaguchi, K. Tamao, A Key Role of Orbital Interaction in the Main Group Element-containing π-Electron Systems, Chem. Lett. 34 (2004) 2–7, doi:10.1246/cl.2005.2.

[2] S. Yamaguchi, K. Tamao, Silole-containing - and -conjugated compounds, (1998) 3693–3702.

[3] R. Chen, R. Zhu, C. Zheng, Q. Fan, W. Huang, Synthesis, characterization and applications of vinylsilafluorene copolymers: New host materials for electroluminescent devices, Sci. China Chem. 53 (2010) 2329–2336, doi:10.1007/s11426-010-4108-7.

[4] S.F. Chen, Y. Tian, J. Peng, H. Zhang, X.J. Feng, H. Zhang, X. Xu, L. Li, J. Gao, Synthesis and characterization of arylamino end-capped silafluorenes for blue to deep-blue organic light-emitting diodes (OLEDs), J, Mater. Chem. C. 3 (2015) 6822–6830, doi:10.1039/C5TC00382B.
[5] X.-Y. Liu, Q.-S. Tian, D. Zhao, Q. Ran, L.-S. Liao, J. Fan, 9-Silafluorene and 9-germafluorene: novel platforms for highly efficient red phosphorescent organic light-emitting diodes, J, Mater. Chem. C. 6 (2018) 8144–8151, doi:10.1039/C8TC02851F.
[6] D. Wang, Q. Liu, Y. Yu, Y. Wu, X. Zhang, H. Dong, L. Ma, G. Zhou, B. Jiao, Z. Wu, R. Chen, Silafluorene moieties as promising building blocks for constructing wide-energy-gap host materials of blue phosphorescent organic light-emitting devices, Sci. China Chem. 58 (2015) 993–998, doi:10.1007/s11426-015-5329-6.
[7] H.P. Martinez, C.D. Grant, J.G. Reynolds, W.C. Trogler, Silica anchored fluorescent organosilicon polymers for explosives separation and detection, J, Mater. Chem. 22 (2012) 2908–2914, doi:10.1039/C2JM15214B.
[8] A. Krishna, D. Sabba, J. Yin, A. Bruno, L.J. Antila, C. Soci, S. Mhaisalkar, A.C. Grimsdale, Facile synthesis of a hole transporting material with a silafluorene core for efficient mesoscopic CH3NH3PbI3 perovskite solar cells, J, Mater. Chem. A. 4 (2016) 8750–8754, doi:10.1039/C6TA01776B.
[9] M. Akhtaruzzaman, Y. Seya, N. Asao, A. Islam, E. Kwon, A. El-Shafei, L. Han, Y. Yamamoto, Donor–acceptor dyes incorporating a stable dibenzosilole π-conjugated spacer for dye-sensitized solar cells, J, Mater. Chem. 22 (2012) 10771–10778, doi:10.1039/C2JM30978E.
[10] F. Gianfaldoni, F. De Nisi, G. Iasilli, A. Panniello, E. Fanizza, M. Striccoli, D. Ryuse, M. Shimizu, T. Biver, A. Pucci, A push–pull silafluorene fluorophore for highly efficient luminescent solar concentrators, RSC Adv. 7 (2017) 37302–37309, doi:10.1039/C7RA08022K.
[11] P. Tang, L. Li, K. Xiang, Y. Li, S. Li, C. Xu, The fluorescent liquid crystal and spiro-silicon bridged compounds based on silafluorene core, J, Organomet. Chem. (2020) 912, doi:10.1016/j.jorganchem.2020.121178.
[12] R. Goy, U.P. Apfel, C. Elleouet, D. Escudero, M. Elstner, H. Görls, J. Talarmin, P. Schollhammer, L. González, W. Weigand, A silicon-heteroaromatic system as photosensitizer for light-driven hydrogen production by hydrogenase mimics, Eur. J. Inorg. Chem. (2013) 4466–4472, doi:10.1002/ejic.201300537.
[13] H. Toyama, M. Nakamura, Y. Hashimoto, S. Fujii, Design and synthesis of novel ROR inverse agonists with a dibenzosilole scaffold as a hydrophobic core structure, Bioorganic Med. Chem. 23 (2015) 2982–2988, doi:10.1016/j.bmc.2015.05.004.
[14] X. Wang, Y.-Z. Hu, A. Chen, Y. Wu, R. Aggeler, Q. Low, H.C. Kang, K.R. Gee, Water-soluble poly(2,7-dibenzosilole) as an ultra-bright fluorescent label for antibody-based flow cytometry, Chem. Commun. 52 (2016) 4022–4024, doi:10.1039/C5CC10347A.
[15] J.J. McDowell, I. Schick, A. Price, D. Faulkner, G. Ozin, Pure blue emitting poly(3,6-dimethoxy-9,9-dialkylsilafluorenes) prepared via nickel-catalyzed cross-coupling of diarylmagnesate monomers, Macromolecules 46 (2013) 6794–6805, doi:10.1021/ma401346y.
[16] Y. Yabusaki, N. Ohshima, H. Kondo, T. Kusamoto, Y. Yamanoi, H. Nishihara, Versatile synthesis of blue luminescent siloles and germoles and hydrogen-bond-assisted color alteration, Chem. - A Eur. J. 16 (2010) 5581–5585, doi:10.1002/chem.200903408.
[17] T. Ureshino, T. Yoshida, Y. Kuninobu, K. Takai, Rhodium-catalyzed synthesis of silafluorene derivatives via cleavage of silicon-hydrogen and carbon-hydrogen bonds, J, Am. Chem. Soc. 132 (2010) 14324–14326, doi:10.1021/ja107698p.
[18] J.M. Breunig, P. Gupta, A. Das, S. Tussupbayev, M. Diefenbach, M. Bolte, M. Wagner, M.C. Holthausen, H.W. Lerner, Efficient access to substituted silafluorenes by nickel-catalyzed reactions of biphenylenes with et2SiH2, Chem. - An Asian J. 9 (2014) 3163–3173, doi:10.1002/asia.201402599.
[19] B. Wei, D. Zhang, Y.H. Chen, A. Lei, P. Knochel, Preparation of Polyfunctional Biaryl Derivatives by Cyclolanthanation of 2-Bromobiaryls and Heterocyclic Analogues Using nBu2LaCl·4 LiCl, Angew. Chemie - Int. Ed. 58 (2019) 15631–15635, doi:10.1002/anie.201908046.
[20] R. Shintani, C. Takagi, T. Ito, M. Naito, K. Nozaki, Rhodium-catalyzed asymmetric synthesis of silicon-stereogenic dibenzosiloles by enantioselective[2+2+2] cycloaddition, Angew. Chemie - Int. Ed. 54 (2015) 1616–1620, doi:10.1002/anie.201409733.
[21] D. Leifert, A. Studer, 9-Silafluorenes via base-promoted homolytic aromatic substitution (BHAS) - The electron as a catalyst, Org. Lett. 17 (2015) 386–389, doi:10.1021/ol503574k.
[22] L. Omann, M. Oestreich, A Catalytic SE Ar Approach to Dibenzosiloles Functionalized at Both Benzene Cores, Angew. Chem. Int. Ed. Engl. 54 (2015) 10276–10279, doi:10.1002/anie.201504066.
[23] L. Xu, S. Zhang, P. Li, Synthesis of silafluorenes and silaindenes via silyl radicals from arylhydrosilanes: Intramolecular cyclization and intermolecular annulation with alkynes, Org. Chem. Front. 2 (2015) 459–463, doi:10.1039/c5qo00012b.
[24] M. Murata, M. Takizawa, H. Sasaki, Y. Kohari, H. Sakagami, T. Namikoshi, S. Watanabe, Synthesis of dibenzosiloles via platinum-catalyzed intramolecular dehydrogenative cyclization of 2-(dialkylsilyl)biaryls, Chem. Lett. 45 (2016) 857–859, doi:10.1246/cl.160415.
[25] X. Du, Y. Zhang, D. Peng, Z. Huang, Base-Metal-Catalyzed Regiodivergent Alkene Hydrosilylations, Angew. Chemie - Int. Ed. 55 (2016) 6671–6675, doi:10.1002/anie.201601197.
[26] Y. Dong, Y. Takata, Y. Yoshigoe, K. Sekine, Y. Kuninobu, Lewis acid-catalyzed synthesis of silafluorene derivatives from biphenyls and dihydrosilanes: Via a double sila-Friedel-Crafts reaction, Chem. Commun. 55 (2019) 13303–13306, doi:10.1039/c9cc07692a.
[27] M. Murai, N. Nishinaka, M. Kimura, K. Takai, Regioselective Functionalization of 9,9-Dimethyl-9-silafluorenes by Borylation, Bromination, and Nitration, J, Org. Chem. 84 (2019) 5667–5676, doi:10.1021/acs.joc.9b00598.
[28] J. Rao, C. Zhao, Y. Wang, K. Bai, S. Wang, J. Ding, L. Wang, Achieving Deep-Blue Thermally Activated Delayed Fluorescence in Nondoped Organic Light-Emitting Diodes through a Spiro-Blocking Strategy, ACS Omega 4 (2019) 1861–1867, doi:10.1021/acsomega.8b03296.
[29] X. Xu, K. Bai, J. Ding, L. Wang, Deep-blue emitting poly(2′,3′,6′,7′-tetraoctyl-2,7-spirosilabifluorene) simultaneously with good color purity and high external quantum efficiency, Org. Electron. 59 (2018) 77–83, doi:10.1016/j.orgel.2018.04.046.
[30] X. Xu, X. Li, S. Wang, J. Ding, L. Wang, Deep-blue emitting poly[spiro(dibenzoazasiline-10′{,}9-silafluorene)] for power-efficient PLEDs, J. Mater. Chem. C. 6 (2018) 9599–9606, doi:10.1039/C8TC03074J.
[31] D.W. Hammerstroem, J. Braddock-Wilking, N.P. Rath, Synthesis and characterization of luminescent 2,7-disubstituted silafluorenes, J, Organomet. Chem. 813 (2016) 110–118, doi:10.1016/j.jorganchem.2016.04.004.
[32] R.F. Chen, Q.L. Fan, C. Zheng, W. Huang, A general strategy for the facile synthesis of 2,7-dibromo-9- heterofluorenes, Org. Lett. 8 (2006) 203–205, doi:10.1021/ol0524499.
[33] L. Li, C. Xu, S. Li, Synthesis and photophysical properties of highly emissive compounds containing a dibenzosilole core, Tetrahedron Lett 51 (2010) 622–624, doi:10.1016/j.tetlet.2009.11.074.
[34] Bruker Analytical X-Ray, (2010).
[35] G. Sheldrick, A short history of SHELX, (2008) 112–122.
[36] A.L. Spek, Single-crystal structure validation with the program PLATON, J, Appl. Crystallogr. 36 (2003) 7–13, doi:10.1107/S0021889802022112.